Overexpression of a pH-sensitive nitrate transporter in rice increases crop yields

Xiaorong Fan (范晓荣)[a], Zhong Tang (唐仲)[a], Yawen Tan (谭雅文)[a,b], Yong Zhang (张勇)[a], Bingbing Luo (罗冰冰)[b,c], Meng Yang (杨锰)[d], Xingming Lian (练兴明)[d], Qirong Shen (沈其荣)[b], Anthony John Miller[c,1], and Guohua Xu (徐国华)[a,b,1]

[a]State Key Laboratory of Crop Genetics and Germplasm Enhancement, Nanjing Agricultural University, Nanjing 210095, China; [b]Key Laboratory of Plant Nutrition and Fertilization in Lower-Middle Reaches of the Yangtze River, Ministry of Agriculture, Nanjing Agricultural University, Nanjing 210095, China; [c]Metabolic Biology Department, John Innes Centre, Norwich NR4 7UH, United Kingdom; and [d]National Key Laboratory of Crop Genetic Improvement and National Center of Plant Gene Research (Wuhan), Huazhong Agricultural University, Wuhan 430070, China

Edited by Maarten J. Chrispeels, University of California, San Diego, La Jolla, CA, and approved April 26, 2016 (received for review December 21, 2015)

Cellular pH homeostasis is fundamental for life, and all cells adapt to maintain this balance. In plants, the chemical form of nitrogen supply, nitrate and ammonium, is one of the cellular pH dominators. We report that the rice nitrate transporter *OsNRT2.3* is transcribed into two spliced isoforms with a natural variation in expression ratio. One splice form, OsNRT2.3b is located on the plasma membrane, is expressed mainly in the phloem, and has a regulatory motif on the cytosolic side that acts to switch nitrate transport activity on or off by a pH-sensing mechanism. High OsNRT2.3b expression in rice enhances the pH-buffering capacity of the plant, increasing N, Fe, and P uptake. In field trials, increased expression of OsNRT2.3b improved grain yield and nitrogen use efficiency (NUE) by 40%. These results indicate that pH sensing by the rice nitrate transporter OsNRT2.3b is important for plant adaption to varied N supply forms and can provide a target for improving NUE.

nitrate transporter | pH sensing | nitrogen use efficiency | yield | rice

Intracellular pH is stringently regulated, because most metabolic enzymes can function only within a narrow range of pH. The cytosolic pH is maintained around neutrality, whereas in individual organelles, pH can range from 4.7 (lysosome) to 8.0 (mitochondria) (1). Mammalian cells balance cytosolic pH using Na^+/H^+ exchangers, Na^+–HCO_3^- cotransporters, Cl^-–HCO_3^-, or anion exchangers (AEs) (1). When bacteria face an acid challenge, the proton-pumping respiratory chain complexes or proton-coupled ATPases, and secondary active transporters, such as anion-proton antiporters like the Cl^-/H^+ exchangers, are activated to maintain intracellular pH (2). In alkali conditions, bacterial Na^+/H^+ antiport and the generation and transport of CO_2, HCO_3^-, NH_3, and NH_4^+ are the main strategies for pH homeostasis (2).

In plants, cytosolic pH can vary from 7.3 to 8.0 (3). Plant roots acquire mineral nitrogen (N) as the source for growth as nitrate, ammonium, or both; the total amount and the ratio of the two N forms can determine cellular pH. In plants, the phloem is an important tissue for nutrient, mRNA, and signal transport, acting like a neural network connecting the shoot and root (4–8). Phloem pH homeostasis is important for maintaining the physiological balance of the whole plant, as well as the transport and signaling functions of the tissue.

Rice (*Oryza sativa* L.) is a major crop, feeding almost 50% of the world's population. It has been traditionally cultivated under flooded anaerobic soil conditions, where ammonium is the main N source; however, specialized aerenchyma cells in rice roots can transfer oxygen from the shoots to the roots and release it to the rhizosphere, where bacterial conversion of ammonium to nitrate (nitrification) can occur (9). Nitrification in the waterlogged paddy rhizosphere can result in 25–40% of the total crop N being taken up in the form of nitrate, mainly through a high-affinity transport system (HATS) (10). The uptake of nitrate is mediated by cotransport with protons (H^+) that can be extruded from the cell by plasma membrane H^+-ATPases (11).

In this study, we analyzed the function of a nitrate transporter, OsNRT2.3, with natural variation of its expression in rice cultivars and the cytosolic pH regulatory motif in the protein. The high expression of one of the two splice forms of this protein, OsNRT2.3b, in rice resulted in better adaptation to changes of N supply forms in the environment and strong improvements in growth, yield, and nitrogen use efficiency (NUE). Our results have significant implications for the understanding of cytosolic pH balance in plant adaptation and its importance for crop improvement.

Results

Natural Variation in Two Splice Forms of Rice Nitrate Transporter OsNRT2.3. We have shown that one rice gene encoding a component of nitrate high affinity transport system (HATS), *OsNRT2.3*, produces two different transcripts arising from alternative splicing that we term *OsNRT2.3a* and *OsNRT2.3b* (12, 13). Comparing the two mature *OsNRT2.3* mRNAs shows that the predicted protein products differ by 30 amino acids (*SI Appendix*, Fig. S1 *A* and *B*). *OsNRT2.3a* encodes a plasma membrane protein of 516 amino acids that functions in long-distance nitrate transport in the xylem from root to shoot (12, 14), whereas *OsNRT2.3b* encodes a shorter 486-aa plasma membrane protein expressed moderately in the phloem of the shoot and faintly in the root (12) (*SI Appendix*, Fig. S1*C*).

We evaluated the expression of *OsNRT2.3a* and *OsNRT2.3b* in 10 rice cultivars (*SI Appendix*, Fig. S2 *A* and *B*) with differing N accumulation in their straw and found that under low N supply (0.63 mM NH_4NO_3; *SI Appendix*, Fig. S2*C*), the expression ratio of *OsNRT2.3b* and *OsNRT2.3a* in the straw has a strong corelationship with the N content. We identified two different groups

Significance

Significant progress has been made in our understanding of plant adaptive responses to maintain cellular pH under varied N supply forms. Rice is a plant adapted to grow in waterlogged or dryland environments, in contrast to other crops, such as wheat, soybean, and maize. The nitrate transporter OsNRT2.3b provides a molecular mechanism explaining plant adaptation to the ammonium-nitrate supply shift between the waterlogged and drained soil environments. The sensing of cytosolic pH by OsNRT2.3b can function to improve rice nitrogen use efficiency and pH balance, providing an explanation for plant adaptation to changes in the form of N supply.

Author contributions: X.F., Z.T., A.J.M., and G.X. designed research; X.F., Z.T., Y.T., Y.Z., B.L., and M.Y. performed research; X.F., Z.T., X.L., Q.S., A.J.M., and G.X. analyzed data; and X.F., A.J.M., and G.X. wrote the paper.

The authors declare no conflict of interest.

This article is a PNAS Direct Submission.

Freely available online through the PNAS open access option.

[1]To whom correspondence may be addressed. Email: ghxu@njau.edu.cn or tony.miller@jic.ac.uk.

This article contains supporting information online at www.pnas.org/lookup/suppl/doi:10.1073/pnas.1525184113/-/DCSupplemental.

of the cultivars showing this relationship, but this correlation was missing at 1.25 mM NH_4NO_3, the normal N supply level (*SI Appendix*, Fig. S2*D*).

Functional Characterization of OsNRT2.3a and OsNRT2.3b in *Xenopus* Oocytes. Previous studies have shown a major difference between OsNRT2.3a and OsNRT2.3b, with OsNRT2.3a requiring a partner protein, OsNAR2.1, for functional nitrate transport (13–15). In contrast, OsNRT2.3b does not require the OsNAR2.1 partner protein for nitrate membrane transport (13). To better understand the different properties of OsNRT2.3a and OsNRT2.3b in nitrate uptake, we expressed the two corresponding cDNAs in *Xenopus* oocytes. Oocyte expression is good for detecting the instant and dynamic responses of the transporters to nitrate supply changes by recording fluctuations in cell membrane potential and cytosolic pH. We found that oocytes coinjected with *OsNRT2.3a* and *OsNAR2.1* RNA responded to repeated sequential nitrate treatments with an electrical depolarization of membrane potential, whereas *OsNRT2.3b*-injected oocytes did not show such repeated nitrate-elicited responses (Fig. 1 *A*, *B*, *D*, and *E* and *SI Appendix*, Fig. S3 *A* and *B*).

Double-barreled proton-selective microelectrode measurements revealed decreased cytosolic pH in oocytes during nitrate transport (shown from 6 to 9 min in the recording in Fig. 1*D* and in the first 7 min of the recording in *SI Appendix*, Fig. S3*A*), indicating that nitrate/proton cotransport resulted in cytosolic acidification (14, 16). The nitrate-elicited cytosolic acidification was reversed by washing the oocyte with pH 8 saline. After this alkaline wash, nitrate treatment could once again elicit a depolarization of the membrane potential of the OsNRT2.3b-expressing cells, with a critical threshold cytosolic pH for the response of ∼7.4 (shown from 33 to 41 min in Fig. 1*D* and from 39 to 46 min and from 58 to 62 min in *SI Appendix*, Fig. S3*A*). The relative initial acidic cytosolic pH (∼7.2) of the oocytes treated by a pH 7.0 bath solution also inhibited nitrate transport, but after a wash in pH 8.0 solution, the alkaline cytosolic pH restored nitrate transport (*SI Appendix*, Fig. S3*C*).

We repeated the experiments several times and pooled the data on simultaneous changes (delta) in membrane potential and cytosolic pH elicited by the nitrate treatments (*SI Appendix*, Fig. S3*B*). Statistical analysis indicated that the initial nitrate treatment at alkaline cytosolic pH (7.41 on average) resulted in large nitrate transport, whereas the relative acidic cytosolic pH (7.25 on average) at the beginning of the second nitrate treatment inhibited nitrate transport. This suggests that ∼0.16 pH units of cytosolic acidification prevented the nitrate transport activity of OsNRT2.3b (*SI Appendix*, Fig. S3*B*). There was no significant difference in the transporter activity of OsNRT2.3b at cytosolic pH 7.41 or 7.56 (*SI Appendix*, Fig. S3*B*).

We also observed that the membrane potential response to nitrate treatment at alkaline cytosolic pH, as in Fig. 1*D*, had a different slope than the responses shown in *SI Appendix*, Fig. S3 *A* and *C* at a more acidic cytosolic pH. Interestingly, the oocytes coinjected with *OsNRT2.3a* and *OsNAR2.1* mRNA did not show any pH sensitivity in their nitrate-elicited electrical response (Fig. 1*E*).

Cytosolic pH Regulatory Motif Characterization in OsNRT2.3b Transport. Some AE proteins participate in mammalian cell pH regulation, and regulatory motifs have been identified in their cytoplasmic domains (17–21). The differing sensitivity of OsNRT2.3a and OsNRT2.3b to nitrate transport-elicited changes in cytosolic pH prompted us to

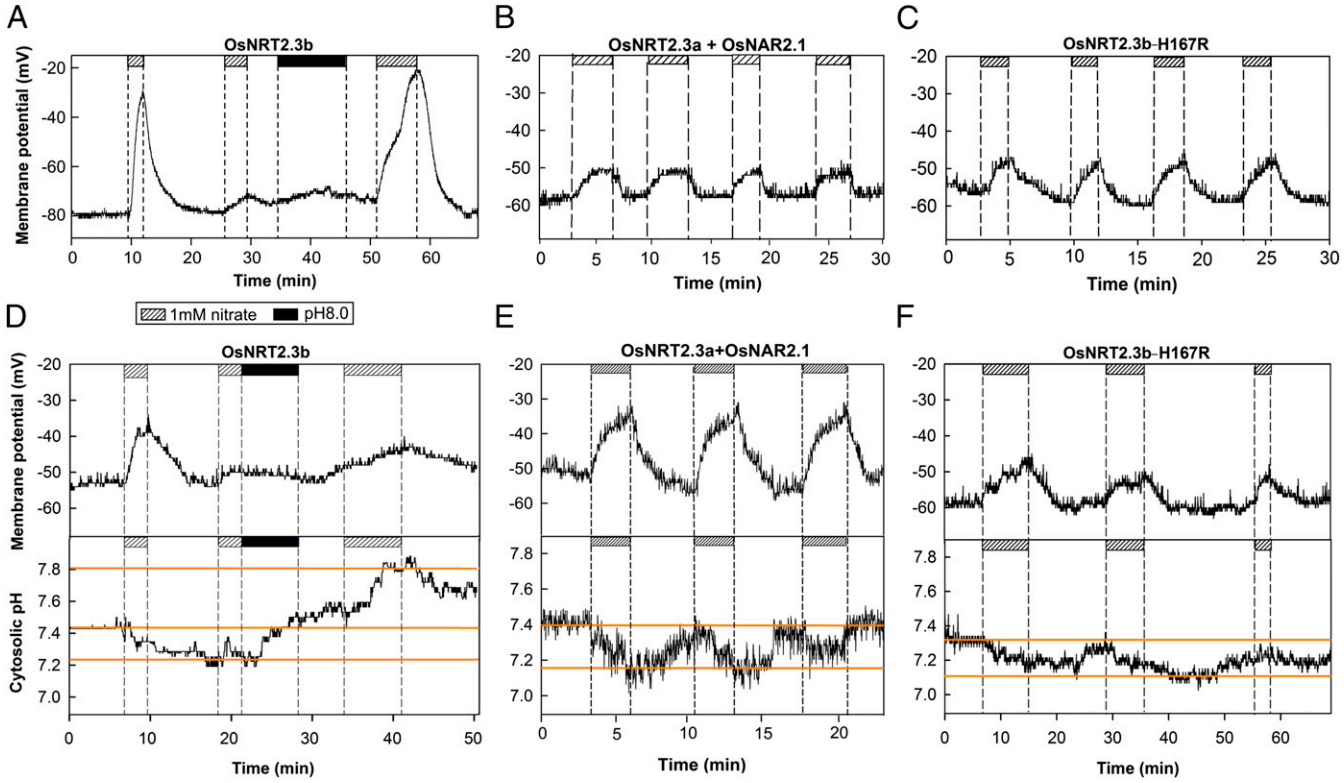

Fig. 1. Functional analysis of OsNRT2.3b, OsNRT2.3a + OsNAR2.1, and H167R transporters expressed in *Xenopus* oocytes. (*A*–*C*) Oocyte plasma membrane potential changes in response to 1 mM nitrate treatment (shaded bar) and pH 8.0 saline wash (black bar) for a cell expressing OsNRT2.3b (*A*), OsNRT2.3a + OsNAR2.1 (*B*), and OsNRT2.3b-H167R mutant (*C*). (*D*–*F*) Double-barreled pH electrode recording of cytosolic pH from oocytes injected with *OsNRT2.3b* treated with 1 mM nitrate (shaded bar) and pH 8.0 saline (black bar) washing (*D*), with *OsNRT2.3a* + *OsNAR2.1* (*E*), and with *OsNRT2.3b*-H167R (*F*) treated with 1 mM nitrate (shaded bar).

look for possible pH-sensing motifs. Using software for scanning protein fingerprints (www.ebi.ac.uk/Tools/pfa/fingerprintscan/), we identified two AE motifs (VYEAIHKI and LGLISGMTG) in the proteins of OsNRT2.3a and OsNRT2.3b. Analysis of some plant NRT2 protein sequences showed that these AE motifs were present in nitrate transporters from several different plant species (*SI Appendix*, Table S2).

The membrane topographical characteristic of OsNRT2.3a and OsNRT2.3b were predicted using transmembrane protein software (*SI Appendix*, Table S1). As displayed by TMPred (www.ch.embnet.org/software/TMPRED_form.html), the software predicted that VYEAIHKI is facing the cytosolic side in OsNRT2.3b, whereas it is at the external side in OsNRT2.3a (*SI Appendix*, Fig. S4 *G* and *H*); however, the LGLISGMTG motif is predicted at the external (LGL) and transmembrane (ISGMTG) regions in OsNRT2.3b (*SI Appendix*, Fig. S4 *G* and *H*). Therefore, we focused on detecting the role of VYEAIHKI in sensing the cytosolic pH in OsNRT2.3b.

Histidine residues are important for pH sensing (22). Given that the H residue of VYEAIHKI for the OsNRT2.3b protein might be located in the border between cytosol and transmembrane (*SI Appendix*, Fig. S4*G*), and VYEAI is predicted as transmembrane, we made a single site mutation (H167R) in this motif. Interestingly, OsNRT2.3b lost the cytosolic pH regulation by this mutation, even after repeated cycles of nitrate treatment (Fig. 1 *C* and *F*). The cytosolic pH decreased from 7.4 to ∼7.2 with nitrate treatments, but the electrical depolarization in membrane potential still occurred despite acidification by repeated nitrate treatments. It was no longer necessary to restore the membrane response to nitrate with an alkaline wash (Fig. 1 *C* and *F*).

When oocytes were incubated in ^{15}N-nitrate for only 4 h, the effect of H167R mutation on nitrate transport was clear, with the comparison of H167R and wild-type (WT) OsNRT2.3b showing that the mutation resulted in much greater nitrate accumulation (Fig. 2*A*). This also might result from changes in the K_m of H167R protein for nitrate, given that the affinity was significantly increased when the membrane potential was in the −40 to −60 mV range, compared with OsNRT2.3b (*SI Appendix*, Fig. S5*D*). Thus, the H167R protein may be more efficient in nitrate transport in 4-h ^{15}N-NO_3^- uptake experiments compared with OsNRT2.3b (Fig. 2*A*). After an 8-h ^{15}N-NO_3^- incubation, the difference in nitrate accumulation between the two forms of the transporter had disappeared, suggesting that after the longer incubation, the accumulation of nitrate had reached a maximum in the oocytes (Fig. 2*A*).

The affinity of OsNRT2.3b, the H167R mutation, and OsNRT2.3a for nitrate showed similar K_m values for NO_3^- at ∼0.45 mM when the membrane potential exceeded −100 mV (*SI Appendix*, Fig. S5), the normal level for plant cells (23–25). For OsNRT2.3a and H167R, nitrate K_m increased as the potentials decreased from −100 mV to −40 mV (*SI Appendix*, Fig. S5*D*). The point mutation H167R influenced the voltage dependence of the turnover rate (*SI Appendix*, Fig. S5), with a change in charge density altering the voltage dependence of both V_{max} and K_m for nitrate (*SI Appendix*, Fig. S5 *D* and *E*). H167R behaves like the other spliced form of the transporter, OsNRT2.3a.

To confirm that the VYEAIHKI motif of OsNRT2.3a and OsNRT2.3b is indeed located on different sides of the plasma membrane, we performed flow cytometry with an anti-His(6)FITC–tagged antibody to determine the membrane topology in rice protoplasts. The 6-His signal of OsNRT2.3b H167 was found to be much lower at the external surface compared with cytosolic face signal obtained after intracellular fixation and permeabilization of the rice protoplasts (Fig. 2*B* and *SI Appendix*, Fig. S4 *C* and *D*). The opposite pattern was found in the 6-His signal of OsNRT2.3a H197, however; that is, the external surface of intact protoplast had more signal (Fig. 2*B* and *SI Appendix*, Fig. S4 *E* and *F*). These FITC data (Fig. 2*B*) confirm that the pH-sensing motif VYEAIHKI around residue H167 in OsNRT2.3b is on the cytosolic face (*SI Appendix*, Fig. S4*G*), but for OsNRT2.3a, the same motif is on the external face of the protoplast (*SI Appendix*, Fig. S4*H*).

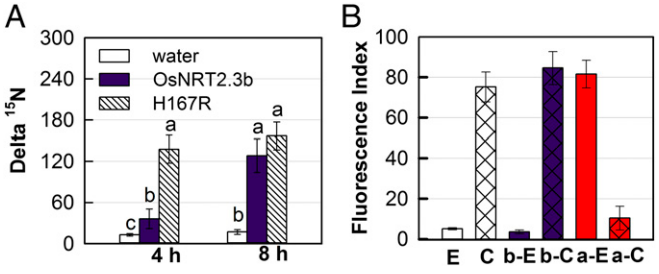

Fig. 2. Nitrate uptake assay in oocytes and the membrane orientation of the OsNRT2.3a/OsNRT2.3b pH-sensing motif in rice protoplasts determined by flow cytometry. (*A*) ^{15}N-NO_3^- uptake by the oocytes injected with water, *OsNRT2.3b*, and H167R mutant mRNAs. Values are mean ± SE (n = 15). Cell viability was tested by electrophysiology after the incubation experiments. a, b, and c above bars indicate significant differences between mRNA and water injected cells ($P < 0.05$) estimated by one-way ANOVA. (*B*) Fluorescence index (FI) of OsNRT2.3b and OsNRT2.3a samples shown in *SI Appendix*, Fig. S4. FI is calculated as fluorescence protoplast number/total protoplast number. 6x-His tag–expressing protoplasts served as positive controls as shown: E for its external side fluorescence within only W5 solution and C for cytosolic side fluorescence with permeabilization buffer in W5 solution; b-E and b-C for external and cytosolic side fluorescence of OsNRT2.3b, respectively; and a-E and a-C for external and cytosolic side fluorescence of OsNRT2.3a, respectively.

High Expression of *OsNRT2.3b* Improved Rice Growth and NUE. To investigate OsNRT2.3b function in rice NUE, we tested the effect of overexpressing *ONRT2.3a*, *OsNRT2.3b*, and the H167R mutated *OsNRT2.3b* in transgenic rice plants (*Oryza sativa* L ssp. Japonica, Nipponbare). We generated overexpression lines for *OsNRT2.3b* (O1, O2, O4, and O8), *OsNRT2.3a* (a-O1 and a-O2), and H167R (H167R2 and H167R4) (Fig. 3 and *SI Appendix*, Fig. S6 *A–C* and Tables S3 and S4). We backcrossed *OsNRT2.3b* overexpression lines with the WT to prove genetically that the phenotype of O8 line is linked to *OsNRT2.3b* overexpression in pot and field experiments (*SI Appendix*, Fig. S6*D*). We determined that the transgenic DNA insertion sites were in the noncoding regions of the genome (*SI Appendix*, Fig. S7 *E* and *F*). We observed that *OsNRT2.3b*-overexpressing plants showed improved growth, yield, and NUE relative to the WT, but not to the *OsNRT2.3a*- and H167R- overexpressing plants (Fig. 3 and *SI Appendix*, Fig. S6). We repeated these experiments in both pot (Fig. 3 *A* and *B* and *SI Appendix*, Fig. S6 *A* and *B*) and field experiments (*SI Appendix*, Figs. S6*C*, S8, and S9) under semitropical and tropical climate conditions (*SI Appendix*, Tables S5 and S6). Furthermore, irrespective of the promoter used to drive the overexpression [Ubiquitin (Ubi), O1 and O2 lines or 35S, O4 and O8 lines], we found the same phenotype for *OsNRT2.3b*-overexpressing plants under adequate and deficient N fertilizer supplies (*SI Appendix*, Figs. S8 and S9 and Table S6).

Overexpression was checked at the mRNA and protein level and found to be increased for *OsNRT2.3a*, *OsNRT2.3b*, and H167R, with the same enhanced expression pattern in the transformed lines (Fig. 3 *A* and *B*). We observed strong expression of both *OsNRT2.3b* and H167R in root and leaf cells in the transgenic lines by RNA in situ blotting (*SI Appendix*, Fig. S7*G*). This overexpression pattern could improve plant nitrate uptake from the external environment and delivery to the shoot. We did not find any significant yield or NUE increase in the *OsNRT2.3a*- and H167R-overexpressing lines relative to the Nipponbare WT, however (Fig. 3 and *SI Appendix*, Figs. S6 and S8). Furthermore, we found the same improvement by *OsNRT2.3b* overexpression in a high-yielding and high-NUE cultivar background (*SI Appendix*, Fig. S9).

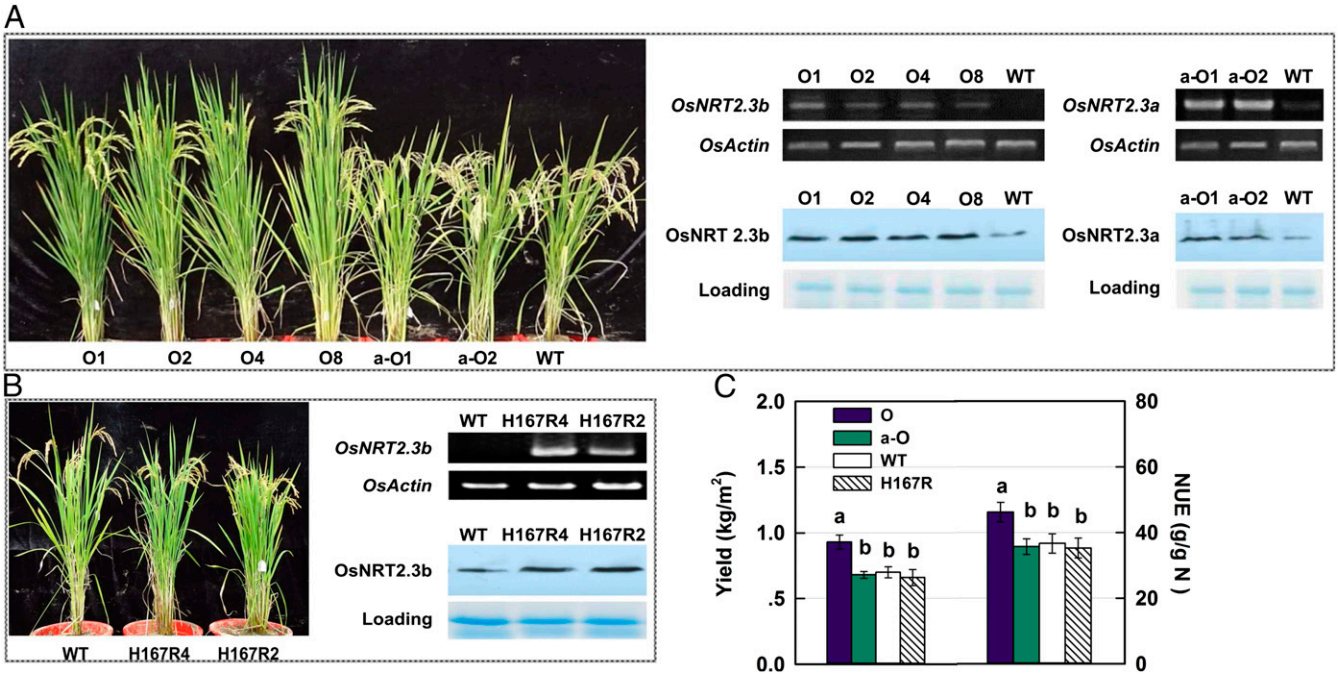

Fig. 3. Growth, yield, and NUE of *OsNRT2.3b*, *OsNRT2.3a*, and H167R mutation overexpressing lines. (*A*) Phenotypes and transcriptional and translational expression of *OsNRT2.3b*- and *OsNRT2.3a*-overexpressing lines and Nipponbare WT. (*B*) Phenotypes and transcriptional and translational expression of WT and *OsNRT2.3b*-H167R mutant-overexpressing lines. (*C*) Average grain yield and NUE of *OsNRT2.3b*- (O), *OsNRT2.3a*- (a-O), and H167R- (H167R) overexpressing lines and WT in field plots. RT-PCR with the specific primers (*SI Appendix*, Table S10) and Western blot analyses with monoclonal antibodies were performed to identify protein expression levels. (NUE = grain yield/applied N fertilizer.) Values are mean ± SE ($n = 3$). a and b above bars indicate significant differences ($P < 0.05$) between the transgenic lines and WT estimated by one-way ANOVA.

The grain yield of overexpressing lines showed that OsNRT2.3b improved rice growth to give 35–54% more in the O8 line under varied N supplies (Fig. 3*C* and *SI Appendix*, Fig. S8 and Table S6) in field plots. With only one-quarter of the normal local N fertilizer application (75 kg N per ha), the grain yield of O8 could reach that of WT under a more typical N supply (300 kg N per ha) (*SI Appendix*, Fig. S8 and Table S6). The most obvious improvement by *OsNRT2.3b* overexpression, but not by *OsNRT2.3a* or H167R overexpression, was in panicle size, including increased length, number of primary and secondary rachises (*SI Appendix*, Fig. S6*B*), number of seeds per panicle, and seed setting rates (*SI Appendix*, Table S6) under different N treatments.

Calculating the NUE using the yield produced divided by the N fertilizer supply, the value for O8 and other *OsNRT2.3b*-overexpressing plants was increased by 26–47% at 300 kg N per ha compared with WT, *OsNRT2.3a*, and H167R lines. The NUE was increased in overexpressor O8 up to 80% at 75 kg N per ha (Fig. 3*C* and *SI Appendix*, Fig. S8 and Table S6). In contrast, the *OsNRT2.3b*- and H167R-overexpressing lines did not show any N-dependent improvement in yield or NUE (Fig. 3*C* and *SI Appendix*, Fig. S8 and Table S6).

Characterization of *OsNRT2.3b* Overexpression in Rice Showing a Function in pH Regulation. We measured the effect of *OsNRT2.3b*, *OsNRT2.3a*, and H167R overexpression on the $^{15}N\text{-}NO_3^-$ and $^{15}N\text{-}NH_4^+$ influx of hydroponically grown rice at pH 6 (Fig. 4*A*). The NO_3^- influx rate was increased significantly over that in WT in all transgenic lines except the *OsNRT2.3a* overexpressor (Fig. 4*A* and *SI Appendix*, Fig. S10*A*). In contrast, *OsNRT2.3b*, *OsNRT2.3a*, and H167R overexpression had no significant effect on short-term $^{15}N\text{-}NH_4^+$ influx (Fig. 4*A* and *SI Appendix*, Fig. S10*A*). Compared with WT, the *OsNRT2.3b*, *OsNRT2.3a*, and H167R overexpressors showed less $^{15}N\text{-}NH_4{}^{15}NO_3$ in 5-min uptake experiments; in this short duration of N uptake, NH_4^+ in NH_4NO_3 was the main form of N influx into the root (Fig. 4*B* and *SI Appendix*, Fig. S10*B*). Compared with WT, the O8 line and other *OsNRT2.3b* overexpressors showed more $^{15}N\text{-}^{15}NH_4NO_3$ and total N uptake at pH 6 and pH 4; however, the *OsNRT2.3a* lines showed similar uptake and the H167R lines showed less uptake (Fig. 4 *B* and *C* and *SI Appendix*, Fig. S10*B*). An exception was line a-O1, which was lower than WT at pH 4 (*SI Appendix*, Fig. S10*C*). The same pattern was seen for $^{15}N\text{-}^{15}NH_4{}^{15}NO_3$ uptake (Fig. 4 *B* and *C* and *SI Appendix*, Fig. S10 *B* and *C*). Expression in oocytes showed that OsNRT2.3b does not transport NH_4^+ irrespective of the presence of nitrate (*SI Appendix*, Fig. S11 *A* and *B*).

The phloem sap pH in overexpressor line O8 (collected as shown in *SI Appendix*, Fig. S12) was 7.1, whereas that of WT and H167R2 was near 8 under NO_3^- supply. In contrast O8 phloem sap pH was 6.8, but WT and H167R2 was ~7.4, under NH_4^+ supply (Fig. 5*A*). In nonsterile hydroponic culture with NH_4^+, some microbial nitrification produces low concentrations of nitrate (26); therefore, *OsNRT2.3b* overexpression may improve growth even under NH_4^+ supply, owing to small amounts of nitrate in the solution. It is known that an acidic phloem sap benefits P and Fe translocation to the leaf (27). We found that the relatively low phloem sap pH increased total P and Fe in the leaves of the *OsNRT2.3b* lines compared with H167R2 and WT (Fig. 5*B* and *SI Appendix*, Fig. S13); however, phloem sap pH is a relative comparison, considering that the sample had passed through an insect.

The increases in N uptake and P and Fe content could benefit C metabolism in the *OsNRT2.3b*-overexpressing lines. Microarray and confirmatory quantitative RT-PCR showed that decreased expression of the genes involved in the photorespiratory pathway in line O8 relative to WT and H167R2 (*SI Appendix*, Fig. S14). Compared with WT and H167R-overexpressing lines, the *OsNRT2.3b* lines showed the same photosynthesis rate per unit of leaf area, higher total photosynthesis per leaf and

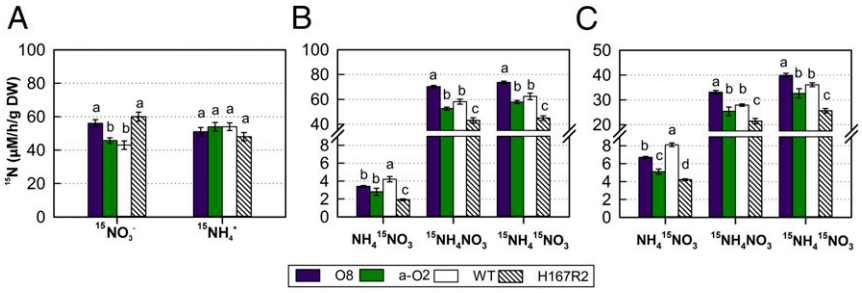

Fig. 4. Effects of *OsNRT2.3b*, *OsNRT2.3a*, and H167R overexpression on the root influx of $^{15}NO_3^-$ and $^{15}NH_4^+$ at pH 6 and 4 for 5 min. (*A*) The root ^{15}N influx rate at 2.5 mM NO_3^- [supplied as $Ca(NO_3)_2$] or NH_4^+ (supplied as NH_4Cl) at pH 6.0. (*B* and *C*) The root ^{15}N influx rate in $NH_4{}^{15}NO_3$, $^{15}NH_4NO_3$, and $^{15}NH_4{}^{15}NO_3$ supply at pH 6 (*B*) and pH 4 (*C*). The ^{15}N influx was measured for 5 min. Values are mean ± SE (n = 5). a, b, and c above bars indicate significant differences ($P < 0.05$) between the transgenic lines and WT for the same treatment estimated by one-way ANOVA.

intercellular CO_2 concentration, and lower photorespiratory rate (*SI Appendix*, Fig. S15).

Discussion

The recently released database of rice genomic variations (28) identifies single nucleotide polymorphisms and insertions/deletions in 1,479 rice accessions, including both landraces and improved varieties from 73 countries. The cross-population likelihood method (XP-CLR) was used to identify genetic selection signals. The XP-CLR data for these rice accessions showed that only *OsNRT2.3* of the rice nitrate transporter genes was under selection pressure during evolution and was much stronger in *Indica II* compared with *Indica I* rice cultivars (29). Our expression data confirm the XP-CLR results, showing that there were two selection patterns in rice; that is, one group of rice cultivars had selection pressure on the expression ratio of *OsNRT2.3b* to *OsNRT2.3a* linking with N accumulation, whereas the other group lost this selection. The division of rice cultivars in the responses of *OsNRT2.3b* and *OsNRT2.3a* expression to N supply may result from their different growth and cultivation conditions (29).

Comparison of the predicted protein sequences of HvNRT2.1 and the rice and *Arabidopsis* NRT2s using the FingerPRINTScan software (www.ebi.ac.uk/Tools/pfa/fingerprintscan/) revealed AE family signature motifs in both OsNRT2.3a/b and AtNRT2.7 (30). Because AE proteins participate in pH regulation (17, 31), these motifs may be important for pH sensing in the plant nitrate transporters. In view of the critical importance of histidine residues within pH-sensing motifs (22), we chose the histidine within the VYEAIHKI as a target for single site mutagenesis, and it was changed to an arginine residue. The functional analysis in oocytes showed that the single amino acid site mutation, H167R of OsNRT2.3b, had lost cytosolic pH regulation even after repeated cycles of nitrate treatment (Fig. 1*D*). This result suggests the VYEAIHKI motif as a pH-regulation site in the sequence of some plant nitrate transporters.

Along with the external and cytosolic pH, the proton gradient for nitrate transport also depends on the membrane potential. Nitrate transport is driven by the electrochemical gradient for protons, and our data in oocytes suggest that it is this parameter, as well as cytosolic pH, that can directly regulate OsNRT2.3b nitrate transport activity (Fig. 1*D* and *SI Appendix*, Fig. S3 *A–C*).

The form of N supply for plants is well known to influence plant pH balance (32). The pH-sensing switch of OsNRT2.3b is a key factor, providing an explanation for the phenotype of *OsNRT2.3b* transgenic plants, because *OsNRT2.3a* and the H167R mutation lines had lost this super phenotype and behaved like WT (Figs. 3–5 and *SI Appendix*, Figs. S6, S8, and S9 and Table S6). A synergism between ammonium and nitrate nutrition in plants has been widely observed. The simultaneous availability of nitrate and ammonium enhances the uptake of ammonium and total N influx, whereas this mix depresses short-term nitrate influx compared with either ammonium or nitrate alone in rice (33). This synergism between N supply forms was enhanced by overexpression of *OsNRT2.3b*, with increased ammonium and total N influx compared with WT (Fig. 4 *A–C* and *SI Appendix*, Fig. S10 *A–C*). The influx and assimilation of nitrate and ammonium requires cytosolic pH homeostasis, with regulation partly contributed by the OsNRT2.3b sensing motif. The proton-cotransport mechanism for the entry of nitrate into cells provides cytosolic acidification, whereas ammonium transport can cause an alkalinization (34), which may enhance proton-coupled nitrate transport. The assimilation of ammonium produces at least one H^+ per NH_4^+, whereas NO_3^- assimilation produces almost one OH^- per NO_3^- (32). Either H^+ or OH^- produced in excess of that required to maintain cytoplasmic pH is exported from the cell in an energy-requiring step (e.g., plasma membrane H^+ pumping ATPase) (11, 16). The advantages of a mixed NO_3^- and NH_4^+ supply for plant pH balance have long been recognized (32, 35). The short-term synergism between ammonium and nitrate to maintain cytosolic pH can explain the measured increase in ^{15}N-NH_4^+ uptake when the plant was supplied with a mixed N source (Fig. 4 *B* and *C*).

In WT plants, *OsNRT2.3b* expression was low (12, 13) (*SI Appendix*, Fig. S7*G*). The transgenic plants with *OsNRT2.3b* overexpression driven by strong promoters had more general tissue expression (*SI Appendix*, Fig. S7*G*). The synergism between ammonium and nitrate was enhanced by overexpression of the pH-sensing transporter OsNRT2.3b more generally in cells, but this did not occur in *OsNRT2.3a* or H167R overexpressors when the pH sensor was lost. The lower N uptake in the H167R lines may be related to (*i*) the changes in K_m and V_{max} for nitrate introduced by the H167R mutation from OsNRT2.3b, making the protein behave more like OsNRT2.3a (*SI Appendix*, Fig. S5); (*ii*) alterations of expression pattern by different promoters; (*iii*) formation of a homodimer by the transporter, impairing native OsNRT2.3b function; and (*iv*) inactivation of the pH sensor along with flipping the location of the protein on the membrane by the H167R substitution. More work is needed to uncover the full phenotype of H167R lines.

Because nitrate assimilation depends on photorespiration (36, 37), the relationship between the assimilation of nitrate and

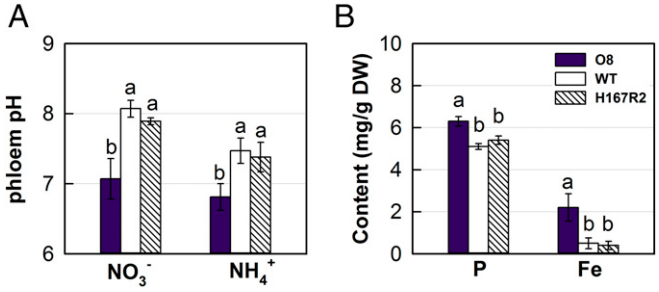

Fig. 5. Effects of *OsNRT2.3b* and H167R overexpression on phloem pH and P and Fe content. (*A*) Phloem pH under 2.5 mM NO_3^-[supplied as $Ca(NO_3)_2$] or NH_4^+(supplied as NH_4Cl). (*B*) Total P and Fe content in leaves measured by ion chromatography analysis. Values are mean ± SE (n = 5). a, b, and c above bars indicate significant differences ($P < 0.05$) between the transgenic lines and WT estimated by one-way ANOVA.

ammonium and photorespiration (36–38) is closely coupled to the shuttling of malate between the cytoplasm and chloroplast to balance pH (39). Compared with the WT and H167R overexpressors, the *OsNRT2.3b* overexpressors had a higher intercellular CO_2 level and a lower photorespiratory rate in the leaves (*SI Appendix*, Fig. S15 *C* and *D*), which might result in increased biomass and grain yields (40, 41) (Fig. 3*C* and *SI Appendix*, Fig. S6 *A–C*). Why *OsNRT2.3b* overexpression would increase leaf intercellular CO_2 remains unclear, however. One possible explanation may be the linkage of nitrate assimilation and photorespiration, given that nitrate in comparison with ammonium nutrition is reported to increase photorespiration under high light (36). *OsNRT2.3b* overexpression increased the uptake of ammonium more than that of nitrate (Fig. 4 *B* and *C*), which might result in a lower photorespiratory rate. Another possible explanation is the strong ectopic expression of *OsNRT2.3b* in leaf mesophyll cells (*SI Appendix*, Fig. S7*G*), which may enhance the cytosolic pH balance in leaf mesophyll cells and influence the intercellular dissolved CO_2 level (40).

In conclusion, the present study shows how overexpression of the cytosolic pH-sensing motif from one side of the membrane to the other can alter pH homeostasis to benefit the rice plant to improve yield and NUE. The improved pH homeostasis may enable plants to adapt to growth environment changes and the ammonium-nitrate shift between waterlogged and drained soils.

Materials and Methods

Functional Analysis in Oocytes. Oocyte preparation, mRNA synthesis and injection, ^{15}N-nitrate uptake, and electrophysiology are described in *SI Appendix*.

Transgenic Plants. Two lines of T7 *OsNRT2.3a*-overexpressing plants (a-O1 and a-O2), four lines of T7 *OsNRT2.3b*- overexpressing plants (O1, O2, O4, and O8), and two lines of T7 H167R overexpressing plants (H167R2 and H167R4) were used in the experiments (*SI Appendix*, Tables S3 and S4). The transformation process and all of the other experiments are described in *SI Appendix*.

ACKNOWLEDGMENTS. We thank Ping Wu (Zhejiang University) for support in the field experiments in Changxing; Yu Liu for part of the ^{15}N analysis; Xiaorong Fan for some of the oocyte experiments, ^{15}N analyses in plants, and phloem sap collection at the John Innes Centre; Xiudong Xia and Shengyuan Li (Nanjing Agricultural University) for the field experiments; I. Bedford (John Innes Centre) for the leaf hopper experiments; and Ali Pendle (John Innes Centre) for technological support in the RNA in situ hybridization. Research in China was funded by the 973 Program (Grant 2011CB100300), the National Natural Science Foundation, the Transgenic Project (Grant 2016ZX08001003-008), the 111 Project (Grant 12009), the Innovative Research Team Development Plan of the Ministry of Education of China, and the Priority Academic Program Development of the Jiangsu Higher Education Institutions project. A.J.M. is supported by Grants BB/J004553/1 and BB/L010305/1 from the Biotechnology and Biological Sciences Research Council and the John Innes Foundation.

1. Casey JR, Grinstein S, Orlowski J (2010) Sensors and regulators of intracellular pH. *Nat Rev Mol Cell Biol* 11(1):50–61.
2. Krulwich TA, Sachs G, Padan E (2011) Molecular aspects of bacterial pH sensing and homeostasis. *Nat Rev Microbiol* 9(5):330–343.
3. Martinière A, Desbrosses G, Sentenac H, Paris N (2013) Development and properties of genetically encoded pH sensors in plants. *Front Plant Sci* 4:523.
4. Molnar A, et al. (2010) Small silencing RNAs in plants are mobile and direct epigenetic modification in recipient cells. *Science* 328(5980):872–875.
5. Dunoyer P, et al. (2010) Small RNA duplexes function as mobile silencing signals between plant cells. *Science* 328(5980):912–916.
6. Wu S, Gallagher KL (2012) Transcription factors on the move. *Curr Opin Plant Biol* 15(6):645–651.
7. Wang A (2015) Dissecting the molecular network of virus-plant interactions: The complex roles of host factors. *Annu Rev Phytopathol* 53:45–66.
8. Notaguchi M, Higashiyama T, Suzuki T (2015) Identification of mRNAs that move over long distances using an RNA-Seq analysis of *Arabidopsis/Nicotiana benthamiana* heterografts. *Plant Cell Physiol* 56(2):311–321.
9. Li YL, Fan XR, Shen QR (2008) The relationship between rhizosphere nitrification and nitrogen-use efficiency in rice plants. *Plant Cell Environ* 31(1):73–85.
10. Kirk GJD, Kronzucker HJ (2005) The potential for nitrification and nitrate uptake in the rhizosphere of wetland plants: A modelling study. *Ann Bot (Lond)* 96(4):639–646.
11. Zhu Y, et al. (2009) Adaptation of plasma membrane $H^{(+)}$-ATPase of rice roots to low pH as related to ammonium nutrition. *Plant Cell Environ* 32(10):1428–1440.
12. Tang Z, et al. (2012) Knockdown of a rice stelar nitrate transporter alters long-distance translocation but not root influx. *Plant Physiol* 160(4):2052–2063.
13. Feng H, et al. (2011) Spatial expression and regulation of rice high-affinity nitrate transporters by nitrogen and carbon status. *J Exp Bot* 62(7):2319–2332.
14. Yan M, et al. (2011) Rice OsNAR2.1 interacts with OsNRT2.1, OsNRT2.2 and OsNRT2.3a nitrate transporters to provide uptake over high and low concentration ranges. *Plant Cell Environ* 34(8):1360–1372.
15. Liu X, et al. (2014) Identification and functional assay of the interaction motifs in the partner protein OsNAR2.1 of the two-component system for high-affinity nitrate transport. *New Phytol* 204(1):74–80.
16. Xu G, Fan X, Miller AJ (2012) Plant nitrogen assimilation and use efficiency. *Annu Rev Plant Biol* 63:153–182.
17. Kurschat CE, et al. (2006) Alkaline-shifted pHo sensitivity of AE2c1-mediated anion exchange reveals novel regulatory determinants in the AE2 N-terminal cytoplasmic domain. *J Biol Chem* 281(4):1885–1896.
18. Kopito RR (1990) Molecular biology of the anion exchanger gene family. *Int Rev Cytol* 123:177–199.
19. Alper SL (1991) The band 3-related anion exchanger (AE) gene family. *Annu Rev Physiol* 53:549–564.
20. Tanner MJA (1997) The structure and function of band 3 (AE1): Recent developments (review). *Mol Membr Biol* 14(4):155–165.
21. Bruce LJ, Unwin RJ, Wrong O, Tanner MJA (1998) The association between familial distal renal tubular acidosis and mutations in the red cell anion exchanger (band 3, AE1) gene. *Biochem Cell Biol* 76(5):723–728.
22. Stewart AK, et al. (2007) Transmembrane domain histidines contribute to regulation of AE2-mediated anion exchange by pH. *Am J Physiol Cell Physiol* 292(2):C909–C918.
23. Fan XR, et al. (2005) A comparison of nitrate transport in four different rice (*Oryza sativa* L.) cultivars. *Sci China Ser C* 48:897–911.
24. Miller AJ (2013) Real time measurement of cytoplasmic ions with ion-selective microelectrodes. *Methods Mol Biol* 953:243–254.
25. Miller AJ, Smith S (2012) Measuring intracellular ion concentrations with multi-barrelled microelectrodes. *Plant Salt Tolerance: Methods and Protocols*, eds Shabala S, Cuin TA (Humana, Totowa, NJ), pp 67–77.
26. Padgett PE, Leonard RT (1993) Contamination of ammonium-based nutrient solutions by nitrifying organisms and the conversion of ammonium to nitrate. *Plant Physiol* 101(1):141–146.
27. Thomine S, Lanquar V (2011) Iron transport and signaling in plants. *Transporters and Pumps in Plant Signaling, Signaling and Communication in Plants*, eds Geisler M, Venema K (Springer, Berlin), pp 99–131.
28. Zhao H, et al. (2015) RiceVarMap: A comprehensive database of rice genomic variations. *Nucleic Acids Res* 43(Database issue, D1):D1018–D1022.
29. Xie W, et al. (2015) Breeding signatures of rice improvement revealed by a genomic variation map from a large germplasm collection. *Proc Natl Acad Sci USA* 112(39): E5411–E5419.
30. Chopin F, et al. (2007) The *Arabidopsis* ATNRT2.7 nitrate transporter controls nitrate content in seeds. *Plant Cell* 19(5):1590–1602.
31. Stewart AK, Kerr N, Chernova MN, Alper SL, Vaughan-Jones RD (2004) Acute pH-dependent regulation of AE2-mediated anion exchange involves discrete local surfaces of the NH2-terminal cytoplasmic domain. *J Biol Chem* 279(50):52664–52676.
32. Raven JA, Smith FA (1976) Nitrogen assimilation and transport in vascular land plants in relation to intracellular pH regulation. *New Phytol* 76(3):415–431.
33. Kronzucker HJ, Siddiqi MY, Glass ADM, Kirk GJD (1999) Nitrate-ammonium synergism in rice: A subcellular flux analysis. *Plant Physiol* 119(3):1041–1046.
34. Kosegarten H, Grolig F, Wieneke J, Wilson G, Hoffmann B (1997) Differential ammonia-elicited changes of cytosolic pH in root hair cells of rice and maize as monitored by 2′,7′-bis-(2-carboxyethyl)-5 (and -6)-carboxyfluorescein-fluorescence ratio. *Plant Physiol* 113(2):451–461.
35. Raven JA (1988) Acquisition of nitrogen by the shoots of land plants: Its occurrence and implications for acid-base regulation. *New Phytol* 109(1):1–20.
36. Bloom AJ (2015) Photorespiration and nitrate assimilation: A major intersection between plant carbon and nitrogen. *Photosynth Res* 123(2):117–128.
37. Rachmilevitch S, Cousins AB, Bloom AJ (2004) Nitrate assimilation in plant shoots depends on photorespiration. *Proc Natl Acad Sci USA* 101(31):11506–11510.
38. Stitt M, et al. (2002) Steps towards an integrated view of nitrogen metabolism. *J Exp Bot* 53(370):959–970.
39. Backhausen JE, Kitzmann C, Scheibe R (1994) Competition between electron acceptors in photosynthesis: Regulation of the malate valve during CO_2 fixation and nitrite reduction. *Photosynth Res* 42(1):75–86.
40. Moroney JV, Jungnick N, Dimario RJ, Longstreth DJ (2013) Photorespiration and carbon concentrating mechanisms: Two adaptations to high O_2, low CO_2 conditions. *Photosynth Res* 117(1-3):121–131.
41. Kebeish R, et al. (2007) Chloroplastic photorespiratory bypass increases photosynthesis and biomass production in *Arabidopsis thaliana*. *Nat Biotechnol* 25(5):593–599.